

Received January 14, 2022, accepted January 27, 2022, date of publication February 1, 2022, date of current version February 10, 2022.

Digital Object Identifier 10.1109/ACCESS.2022.3148398

Exploiting Integrated Demand Response for Operating Reserve Provision Considering Rebound Effects

XIAOMING ZHOU¹, MAOSHENG SANG¹, MINGLEI BAO^{ID 2}, SHENG WANG^{ID 3},
WENQI CUI^{ID 4}, (Graduate Student Member, IEEE), CHENGJIN YE^{ID 1}, (Member, IEEE),
AND YI DING^{ID 1}, (Member, IEEE)

¹College of Electrical Engineering, Zhejiang University, Hangzhou 310063, China

²College of Energy Engineering, Zhejiang University, Hangzhou 310063, China

³State Grid (Suzhou) City and Energy Research Institute Company Ltd., Suzhou 215000, China

⁴Department of Electrical and Computer Engineering, University of Washington, Seattle, WA 98115, USA

Corresponding author: Minglei Bao (baominglei@zju.edu.cn)

ABSTRACT Electricity-driven thermostatically controlled loads (TCLs), e.g., air conditioners (ACs), have been widely utilized in demand response (DR) to provide operating reserve for power systems. However, the rebound effects may occur during the recovery process of DR, which can limit the operating reserve quality of ACs or even affect the reliable operation of power systems. With the community-level smart energy hubs (EH), the traditional electricity-driven TCLs can be expanded into multi-energy driven thermostatically controlled loads (MTCLs), e.g., household radiators. Under this circumstance, integrated demand response (IDR) can be exploited to coordinate the operation of MTCLs and provide more operating reserve resources while mitigating rebound effects. To this end, this paper proposes a two-stage IDR strategy to fully excavate the operating reserve provided by MTCLs. The first stage is to coordinate the energy consumption of ACs and household radiators to maximize the end-users' thermal comfort and mitigate the rebound effects. To quantify the end-users' thermal comfort, a modified predicted percentage of dissatisfied (PPD) index related to thermal environment parameters is introduced and simplified. Based on the energy consumption determined in the first stage, the energy conversion in EH is optimized in the second stage. Through the optimization in these two stages, a series of indices is established to evaluate the operating reserve in terms of aggregate capacity, duration, ramp rate, and smoothness. The case studies demonstrate that the proposed two-stage IDR strategy can provide high-aggregate-capacity and long-duration reserve resources in power systems while mitigating the rebound effects to maintain supply-demand balance and reliable operation of power systems. The analysis results of the test system show that the reserve capacity and duration obtained by the proposed model are 1.85 and 2.61 times those of the model without considering the multi-energy conversion, respectively.

INDEX TERMS Integrated demand response, multi-energy driven thermostatically controlled loads, operating reserve, rebound effect, energy hub, thermal comfort.

I. INTRODUCTION

A. BACKGROUND

With the increasing awareness of environmental protection, a consensus in UN Climate Change Conference (COP26) is formed to accelerate the development of renewable energy, e.g., solar and wind power [1]. However, due

The associate editor coordinating the review of this manuscript and approving it for publication was Vitor Monteiro^{ID}.

to the variability and uncertainty of renewables, power systems need more operating reserves to maintain supply-demand balance [2]–[4]. Operating reserve is the generating capacity available in a short period to avoid power shortage that results from emergencies, such as random failures of the generator and load fluctuations [5]. For guaranteeing the reliable operation of power systems, the electricity-driven thermostatically controlled loads (TCLs) can provide operating reserves by shifting peak electricity demand, e.g.,

demand response (DR) programs [6]. For example, air conditioners (ACs) can be actively controlled to adjust their power consumption by changing their set temperature [7]. The aggregate reserve capacity would be large since the electricity consumption from ACs typically accounts for 35% in China [8]–[10].

However, the rebound effects may occur in the aggregate response of ACs for the provision of operating reserve [8]. This phenomenon is the power rebound that arises when a large number of loads are re-connected to the grid at approximately the same time [9]. Due to temporary changes in ACs' set temperature, the thermal comfort violation of end-users is inescapable during the DR period [5]. Generally, end-users will set their ACs back to their thermal comfort temperature at the end of the required demand response period. This action makes a lot of ACs restart simultaneously and therefore causes a sudden increase in electricity usage [10]. The thermal comfort violation influences the end-users' willingness to participate in DR programs, which will not only decrease the operating reserve capacity but also produce rebound effects. In extreme cases, the increased load current derived from the rebound effects may even lead to the melting of overhead lines, which harms system security considerably [11].

Due to the increasing diversity of energy demands and the development of energy conversion, the smart energy hub (EH), including heating, cooling, and electricity, has been promoted globally [12]. Considering the multi-energy supply in EHs, the traditional electricity-driven TCLs can be expanded into multi-energy driven thermostatically controlled loads (MTCLs). Nowadays, MTCLs containing ACs and household radiators have been widely installed in many areas, e.g., south Australia [12], UK [13], eastern Tehran [14], northeast China [15], and Italy [16]. EH provides the advantage that household radiators can control room temperature through heating/cooling water from EH directly, instead of relying on electricity consumption like traditional ACs. Therefore, the end-users can adjust electricity consumption without reducing thermal comfort. In addition, as multi-energy sources of MTCLs, EH can coordinate the operation of conversion devices for efficiency and economy [13]. Besides, taking advantage of energy conversion between multiple energy sources, EH can implement integrated demand response (IDR) for energy balance and efficiency enhancement [14]. By coordinating the operation of multi-energy conversion devices, IDR with MTCLs could provide more operating reserve capacity while mitigating rebound effects at the same time.

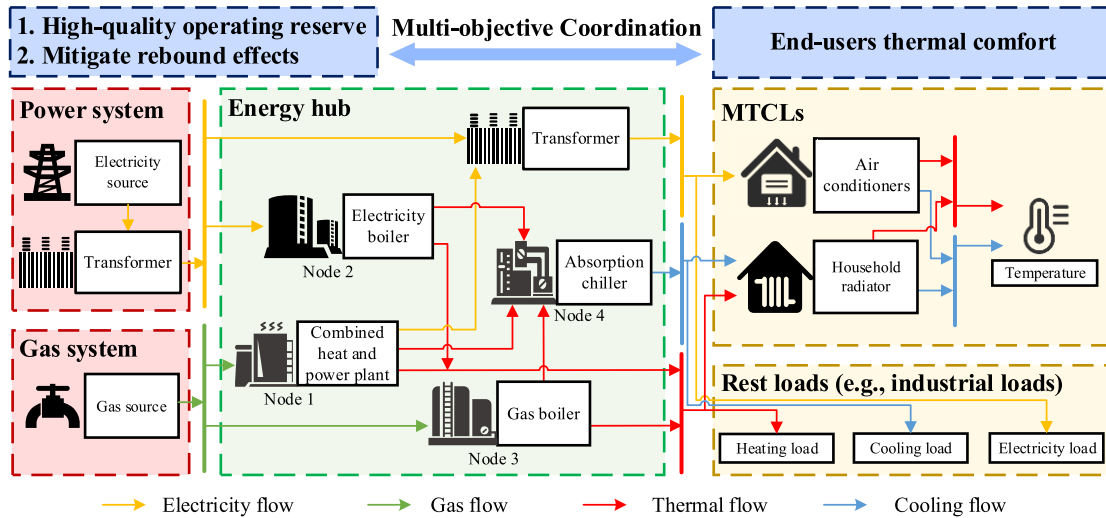
B. LITERATURE REVIEW

At present, extensive research efforts have been dedicated to the operational strategy of DR or IDR. Reference [5] proposed a novel control strategy for the aggregation model of ACs based on the thermal model of the room. Reference [6] proposed a mixed-integer quadratic constrained programming method to solve the computational challenges

produced by the integrated dispatch of generation and load. Reference [7] proposed a novel frequency regulation model of multi-area power systems considering large-scale inverter ACs providing regulation service. Reference [13] proposed an optimal day-ahead scheduling model of EHs considering IDR, cooperative game, and virtual energy storage to maximize the overall benefits of the cooperative alliance. Reference [15] explored interaction patterns for multi-energy demand management and proposed an IDR mechanism for the industrial integrated energy system. The optimization model of the IDR is then established with the objective of minimizing the total dispatch cost. Reference [16] proposed a demand response uncertainty model based on price incentives, which described the relationship between the incentive price and the demand response coefficient. Reference [17] proposed an optimal operation of EHs based on the horizontal complementary substitution and vertical time shift strategy of IDR. Reference [18] proposed a Stackelberg game-based optimization framework for the optimal scheduling of IDR-enabled EHs with uncertain renewable generations. Reference [19] proposed a model for the optimal operation of multi-energy microgrids in the presence of solar photovoltaics, heterogeneous energy storage, and IDR, considering technical and economic ties among the resources. Reference [20] proposed an optimal scheduling model for regional multi-energy prosumers. The formulated objective of this model is to minimize the prosumer's cost of purchasing electricity and natural gas. Reference [21] illustrated that both the responsiveness uncertainty of consumers and output uncertainty of renewable energy sources can be modeled for the sake of designing more preferable incentive strategies of IDR.

These research studies mainly focused on excavating the capacity of operating reserve [5]–[7], [13], [15]–[21]. However, a few pieces of research focus on the other significant characteristics of the operating reserve provision, e.g., duration and smoothness. Admittedly, the operating reserve capacity is important to exploit in IDR. However, there is a lack of consideration on the quality of operating reserve provision, where the short-duration and rebound effects, can limit the potential of IDR for operating reserve provision [22].

Besides, the previous studies mainly focused on the modeling and control of electricity-driven TCLs, i.e., ACs [20], [21]. However, MTCLs can be good candidates to provide operating reserve in IDR programs. Compared with the traditional DR strategy, the IDR strategy is more complicated in terms of both control members and control processes. Specifically, only electricity-driven TCLs, i.e., ACs, are considered in the traditional DR strategy to provide the operating reserve. However, the MTCLs are good candidates to provide operating reserve in IDR strategy, which are more complicated than ACs since the components contained in MTCLs are more diversified and need to be controlled coordinately by satisfying the end-users' thermal comfort. On the one hand, the control process of the traditional DR

**FIGURE 1.** Framework of the proposed IDR strategy.

strategy is relatively simple by directly controlling the power consumption of ACs. However, due to the multi-energy provided by EHs, the control of MTCLs energy consumption relies on the operation optimization of EHs, which needs to be modeled in a unified optimization framework by incorporating both MTCLs and EHs. Moreover, to satisfy end-users' thermal comfort, many studies keep room temperature in a constant interval [20], [21]. However, to characterize the relationship between thermal comfort and operating reserve provision, the thermal comfort violation needs a quantifiable index but is still missing. The comparisons between this paper and previous papers related to the IDR strategy are shown in TABLE 1.

C. CONTRIBUTIONS

To overcome the above challenges, this paper proposes a two-stage IDR strategy to fully excavate the operating reserve provided by MTCLs. The major contributions of this paper are as follows:

1. A two-stage IDR strategy is proposed to fully excavate the operating reserve provided by MTCLs, considering rebound effects. The end-users' thermal comfort and the energy conversion in EH are optimized in the first and second stages respectively. To quantify the end-users' thermal comfort, a modified PPD index is introduced and simplified. According to the proposed IDR strategy, the high-aggregate-capacity and long-duration reserve resources can be provided in power systems while mitigating the rebound effects.
2. To evaluate the quality of operating reserve provided by the IDR strategy, a series of quantitative indices are established in terms of capacity, duration, and smoothness. Based on the quantitative indices, the operating reserve quality can be evaluated more comprehensively, which provides effective guidance for

TABLE 1. Comparisons between this paper and previous research work.

Aspects	Previous research work	Proposed method
Operating reserve provider	Operating reserve provided by ACs [5-7], [16-18], [20, 21] are studied, without considering the multi-energy driven devices. The rebound effects may occur in the demand response of ACs.	The operating reserve provided by multi-energy driven thermostatically controlled loads (MTCLs) is fully excavated. The rebound effects can be avoided by the energy conversion of MTCLs.
Operating reserve quality indices	The capacity of the operating reserve is the main objective to optimize [13], [16-18], but the duration and smoothness are seldom taken into account.	The quality of operating reserve is evaluated more comprehensively in terms of aggregate capacity, duration, and smoothness, which can guide the precise control of MTCLs to excavate high-quality operating reserve.
Thermal comfort satisfaction methods	End-users thermal comfort is satisfied by limiting the temperature to a fixed range [20, 21] without quantification and optimization, which cannot ensure the most comfortable temperature of end-users.	A predicted percentage of dissatisfied (PPD) index is proposed to quantify and optimize the end-users' thermal comfort, which can guarantee the best end-users' thermal comfort.

the precise control of MTCLs to excavate high-quality operating reserve.

II. MULTI-ENERGY THERMAL DYNAMIC MODEL

The framework of the proposed IDR strategy is illustrated in FIGURE 1, which enables MTCLs to provide the operating reserve by utilizing the multi-energy supply from smart EH. Specifically, the EH fed by power and gas systems provides multi-energy (such as electricity, heating, and cooling) for

MTCLs, and then MTCLs are dispatched according to the end-user residential units to provide high-quality operating reserve resources.

In this section, the multi-energy thermal dynamic (METD) model is first developed to describe the operating characteristic of MTCLs and EHs. On this basis, the end-users' thermal comfort and rebound effects can be further analyzed to evaluate the quality of operating reserve in the next section.

A. MODEL OF MTCLs

The METD model is expanded from the classic thermal dynamic model, which has been widely used in previous studies about electric demand response [5]–[7]. To be specific, the classical thermal dynamic model in equation (1) describes the relationship between the room temperature and the output of TCLs, i.e., ACs [5]. In this paper, the MTCLs are considered to provide heating or cooling, including ACs and household radiators. Therefore, the output of electricity-driven TCLs $Q_v(t)$ in (1) is replaced by the total output of MTCLs. On this basis, the METD model can be formulated.

The general thermal dynamic model is shown in equation (1).

$$C_v \frac{dT_v^{in}(t)}{dt} = \frac{1}{R_v} (T_v^{out}(t) - T_v^{in}(t)) + Q_v(t) \quad (1)$$

where, C_v and R_v are the thermal capacity and resistance of room v, respectively. $T_v^{out}(t)$ and $T_v^{in}(t)$ are the ambient temperature and room temperature of room v at time t, respectively. $Q_v(t)$ is the output of TCLs.

In many existing references [24]–[27], only ACs are considered to provide heating in the room. Therefore, the heating output $Q_v(t)$ in room v is related to the operating power of ACs, as shown in equation (2).

$$Q_v(t) = P_v^{AC}(t) \times COP_v^{AC} \quad (2)$$

where, $P_v^{AC}(t)$ is the rated power of AC in room v. COP_v^{AC} is the coefficient of performance (COP) of AC in room v.

In this paper, the MTCLs are considered to provide heating, including ACs and household radiators. Therefore, the output of electricity-driven TCLs $Q_v(t)$ in equation (1) is replaced by the total output of MTCLs, as shown in equation (3).

$$Q_v(t) = [COP_v^{AC} \quad 1] \cdot \begin{bmatrix} P_v^{AC}(t) \\ P_v^{RAD}(t) \end{bmatrix} \quad (3)$$

where, $P_v^{RAD}(t)$ is the energy transfer rate of the household radiator in room v.

In addition, the operation status of ACs and household radiators are also considered. Therefore, the METD model is presented as follows:

$$\begin{aligned} C_v \frac{dT_v^{in}(t)}{dt} &= \frac{1}{R_v} (T_v^{out}(t) - T_v^{in}(t)) \\ &+ m^S \cdot [m_v^{AC}(t) \cdot COP_v^{AC} \quad m_v^{RAD}(t)] \\ &\cdot \begin{bmatrix} P_v^{AC} \\ P_v^{RAD}(t) \end{bmatrix} \end{aligned} \quad (4)$$

$$m^S = \begin{cases} -1 & \text{cooling} \\ 1 & \text{heat} \end{cases} \quad (5)$$

$$m_v^{AC}(t) = \begin{cases} 1, & T_v^{in}(t) > T_{v,+}^{AC}(t) \\ 0, & T_v^{in}(t) < T_{v,-}^{AC}(t) \\ m_v^{AC}(t-1), & \text{otherwise} \end{cases} \quad (6)$$

where, m^S is the operation mode of MTCLs. $m_v^{AC}(t)$ is the operation status (on/off) of the compressors of ACs in room v at time t. $m_v^{RAD}(t) = 1/0$ is the operation status (on/off) of the household radiators in room v at time t.

In equation (4), it should be noticed that the operation forms of these MTCLs are different. Except for the operation status, (on/off) of ACs, the operation status (on/off) of the compressors of ACs is also determined by the difference between the set temperature $T_v^{set}(t)$ and the room temperature $T_v^{in}(t)$. The AC operates cyclically around its set temperature with a dead band of ΔT^{AC} . For example, if the AC is in the cooling mode in summer, it will switch to the on state when the room temperature reaches the upper band ($T_{v,+}^{AC}(t) = T_v^{set}(t) + 0.5 \times \Delta T^{AC}$). Similarly, when the room temperature reaches the lower band ($T_{v,-}^{AC}(t) = T_v^{set}(t) - 0.5 \times \Delta T^{AC}$), it will switch to the standby state. The temperature range between $T_{v,-}^{AC}(t)$ and $T_{v,+}^{AC}(t)$ is defined as the hysteresis band [27], as shown in equation (6). Therefore, the room energy transfer rate not only depends on the operation status (on/off) of these MTCLs, but also depends on the operation status (on/off) of the compressors of ACs.

All of the MTCLs in each end-user residential unit are aggregated and abstracted as a load node. The aggregate power of this node depends on the operation form of these MTCLs, as shown in equation (7) and (8).

$$P_\Omega^{AC}(t) = \sum_v m_v^{AC}(t) \cdot P_v^{AC}, \quad \Omega = E \quad (7)$$

$$P_\Omega^{RAD}(t) = \sum_v m_v^{RAD}(t) \cdot P_v^{RAD}(t), \quad \Omega \in \{C, H\} \quad (8)$$

where, $\Omega \in \{E, G, C, H\}$ represent the energy types (electric/gas/cooling/heating). $P_\Omega^{AC}(t)$ is the aggregate electric power from the EH to ACs. $P_\Omega^{RAD}(t)$ is the aggregate cooling/heating power from the EH to household radiators.

B. MODEL OF EHs

It is important to model the EH for analyzing the IDR strategy as the energy consumption of MTCLs relies on the operation of EHs. Each device in the EH, i.e., combined heat and power plant (CHP), the electricity boiler (EB), the gas boiler (GB), and the absorption chiller (AB), is abstracted as a node. The topology and energy flow variables of the EH are shown in FIGURE 1. The inputs are electricity and natural gas; the outputs are electricity, cooling, and heating. The EH consists of the CHP, the EB, the GB, and the AB, set as devices no.1~4, respectively. Operating constraints and energy flows

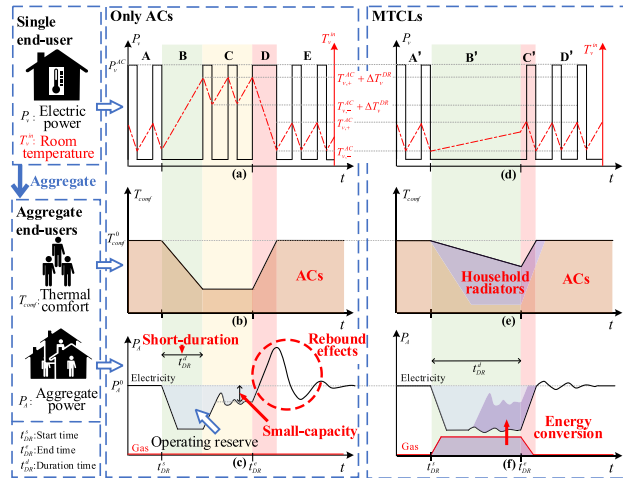


FIGURE 2. Comparisons of operating reserve provided with only ACs and MTCLs.

in the EH can be described as follows [28]:

$$P_{\Omega,i}^{out}(t) = \eta_{\Omega,i} \cdot \sum_j P_{\Omega,ji}^{out}(t), \quad i \in \{1, 2, 3\} \quad (9)$$

$$P_{\Omega,i}^{out}(t) = COP_{\Omega,i} \cdot \sum_j P_{\Omega,ji}^{out}(t), \quad i = 4 \quad (10)$$

$$P_{\Omega}^{EH}(t) = \sum_i P_{\Omega,i}^{out}(t) = P_{\Omega}^{AC}(t) + P_{\Omega}^{RAD}(t) + P_{\Omega}^{REST}(t) \quad (11)$$

where, $i, j \in \{0, 1, 2, 3, 4\}$ represent the devices with the corresponding number in EH. Besides, $i, j = 0$ represents the electric/gas system. $P_{\Omega,i}^{out}(t)$ ($P_{\Omega,ji}^{out}(t)$) is the energy output in energy type Ω of the device i (the device j to the device i). $\eta_{\Omega,i}$ ($COP_{\Omega,i}$) is the energy conversion efficiency (coefficients of performance) in energy type Ω of the device i . $P_{\Omega}^{EH}(t)$ is the aggregate power (electric/cooling/heating) from the EH to MTCLs and the rest loads. $P_{\Omega}^{REST}(t)$ is the multi-energy loads without MTCLs.

III. MITIGATION MECHANISM OF REBOUND EFFECTS WITH MTCLS

Based on the METD model established in Section II, the cause of rebound effects in operating reserve provision with ACs is analyzed in this section. Based on the analysis, the mitigation mechanism of rebound effects with MTCLs is exploited with a specific example. In this example, the MTCLs or ACs are assumed in cooling mode in summer, and the room temperature, thermal comfort, and rebound effects are analyzed respectively as shown in FIGURE 2.

The capacity of the operating reserve is determined by the reduction of the aggregate power of loads. In this paper, the operating reserve is provided by the energy hub and MTCLs. On the MTCL side, under IDR strategy, the ACs will reduce the power consumption by changing the set temperature. Meanwhile, the household radiators will increase the heating/cooling consumption by increasing the gas consumption in the EH. On the EH side, each device of

the EH will operate economically by considering the multi-energy conversion. Therefore, in this paper, the operating reserve is the adjustable power provided by the EH and MTCLs to power systems, which can be represented as a blue area in FIGURE 2(c).

A. THE CAUSE OF REBOUND EFFECTS DURING THE RESERVE PROVISION OF ACs

According to the aggregate consumption power of ACs and the end-users' thermal comfort, the operating reserve provision period can be divided into five parts in this paper, as shown in FIGURE 2(a-c).

1) Part A is the period before operating reserve provision. In part A, the set temperature of ACs is generally low, the power consumption of ACs is large, and the room temperature fluctuates near the set temperature. The end-users' thermal comfort can be satisfied. Considering the difference of each end-users' room temperature and set temperature, the compressors of ACs in different rooms would not be operating at the same time. It is the normal level of aggregate consumption power of ACs.

2) Part B is the infancy stage of operating reserve provision. In part B, the set temperature is raised by end-users to provide operating reserve. The new set temperature is higher than the original set temperature in part A and the current room temperature. The compressors of ACs are in "off" status, and the aggregate power of ACs is small. Although the end-users' thermal comfort will be violated, ACs would not operate and decrease the aggregate power.

3) Part C is the terminal stage of operating reserve provision. In part C, the room temperature gradually rises to the new set temperature, which is higher than the set temperature in part A and E. Therefore, the end-users' thermal comfort will still be violated. The compressors of ACs will be in "on" status, and the aggregate power of ACs will increase in this stage. However, since the set temperature in part C is higher than the original set temperature in part A, the aggregate power of ACs in part C will be slightly lower than that in part A, as shown in FIGURE 2(b) and FIGURE 2(c).

4) Part D is the infancy stage after operating reserve provision. In part D, to satisfy the end-users' thermal comfort, ACs will be operating at the same time. Therefore, the aggregate power will increase in part D, which is the rebound effects [22].

5) Part E is the terminal stage after operating reserve provision. In part E, the end-users' thermal comfort can be satisfied and the aggregate consumption power of ACs will be back to the normal level.

The capacity of rebound effects is defined as the difference of aggregate power consumption between participating in the demand response program or not, which can be described as (12)-(13).

$$P_{RE} = (\alpha_D - \alpha_A) \sum_v P_v^{AC} \quad (12)$$

$$\alpha_A = \alpha_E, \quad \alpha_B = 0, \quad \alpha_C < \alpha_A, \quad \alpha_D = 1 \quad (13)$$

where, P_{RE} is the capacity of rebound effects.

TABLE 2. Situations of operating reserve provision with ACs.

Part	Aggregate consumption of ACs P_{Ω}^{AC}	Aggregate consumption of household radiators P_{Ω}^{RAD}	Set temperature of ACs T_v^{set}	Room temperature T_v^{in}
A	$\alpha_A \sum_v P_v^{AC}$	0	T_v^{comf}	T_v^{comf}
B	$\alpha_B \sum_v P_v^{AC}$	0	$T_v^{comf} + \Delta T_v^{DR}$	Unsolved (not T_v^{comf})
C	$\alpha_C \sum_v P_v^{AC}$	0	$T_v^{comf} + \Delta T_v^{DR}$	Unsolved (not T_v^{comf})
D	$\alpha_D \sum_v P_v^{AC}$	0	T_v^{comf}	Unsolved (not T_v^{comf})
E	$\alpha_E \sum_v P_v^{AC}$	0	T_v^{comf}	T_v^{comf}

α_A , α_B , α_C , α_D , and α_E are the ratios of aggregate consumption during the corresponding period of operating reserve provision. T_v^{comf} is the end-user's thermal comfort temperature in room v . ΔT_v^{DR} is the difference of set temperature between the original status and demand response period.

B. THE OUTLINE TO MITIGATE REBOUND EFFECTS USING MTCLs

As discussed above, serious rebound effects may occur during the reserve provision of ACs. To satisfy the thermal comfort, the end-users set the temperature of ACs back to the thermal comfort temperature at the end of the DR period, leading to a sudden increase in electricity usage. However, the MTCLs, which are quietly different from the ACs by coordinating the multi-energy consumption and conversion to satisfy end-users' thermal comfort, could mitigate the rebound effects significantly during the reserve provision.

In specific, due to the cooling output of household radiators at t_{DR}^s , room temperature has remained below the decreased set temperature at t_{DR}^e , which makes the compressors of ACs stay in the off state in part of a room, as illustrated in FIGURE 2(d).

It is obvious that part A' and part D' are the normal operation states of ACs and end-users' thermal comfort has been satisfied, same as part A and part E, as shown in FIGURE 2(a) and FIGURE 2(d). During operating reserve provision period, due to the output of household radiators, the room temperature will remain near to the comfort temperature, which will extend the part B. Therefore, the time of reduced operating reserve provision (part C) will shrink and even decrease to zero. In this situation, ACs will stay in off status and room temperature will also remain in a comfortable zone, relatively. As shown in FIGURE 2(e) and FIGURE 2(f), part B' is full of the operating reserve provision period with less violation of end-users' thermal comfort and larger provision of operating reserve. Meanwhile, due to the less difference between room temperature and end-users' comfort temperature, quite a few ACs will not operate immediately at the end of operating reserve provision period. Therefore, in part C', the aggregate power of ACs will climb smoothly and with less rebound effects, as shown in FIGURE 2(e).

TABLE 3. Situations of operating reserve provision with MTCLs.

Part	Aggregate consumption of ACs P_{Ω}^{AC}	Aggregate consumption of household radiators P_{Ω}^{RAD}	Set temperature of ACs T_v^{set}	Room temperature T_v^{in}
A'	$\alpha_{A'} \sum_v P_v^{AC}$	0	T_v^{comf}	T_v^{comf}
B'	$\alpha_{B'} \sum_v P_v^{AC}$	Unsolved (not 0)	$T_v^{comf} + \Delta T_v^{DR}$	Unsolved (not T_v^{comf})
C'	$\alpha_{C'} \sum_v P_v^{AC}$	Unsolved (not 0)	T_v^{comf}	Unsolved (not T_v^{comf})
D'	$\alpha_{D'} \sum_v P_v^{AC}$	0	T_v^{comf}	T_v^{comf}

$\alpha_{A'}$, $\alpha_{B'}$, $\alpha_{C'}$, and $\alpha_{D'}$ are the ratios of aggregate consumption during the corresponding period of operating reserve provision.

The aggregate consumption power of MTCLs and the rebound effects can be modeled as TABLE 3 and equation (14)-(15).

$$P_{RE} = (\alpha_{C'} - \alpha_{A'}) \sum_v P_v^{AC} \quad (14)$$

$$\alpha_{A'} = \alpha_{D'}, \quad \alpha_{B'} = 0, \quad \alpha_{C'} < 1 \quad (15)$$

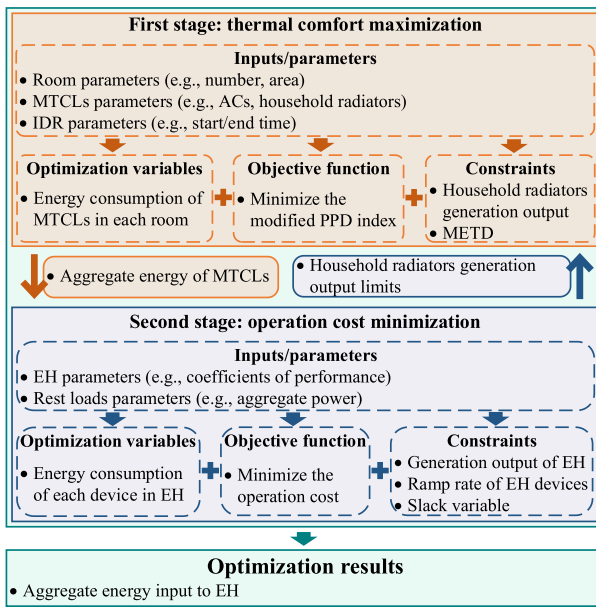
In the same situation, the relationships of parameters of operating reserve provision with ACs and MTCLs can be modeled as:

$$\alpha_A = \alpha_E = \alpha_{A'} = \alpha_{D'}, \quad \alpha_B = \alpha_{B'}, \quad (16)$$

$$\left| T_v^{in}(t) - T_v^{comf} \right| \leq \left| T_v^{in}(t) - T_v^{comf} \right|, \quad t \in [t_{DR}^s, t_{DR}^e] \quad (17)$$

Therefore, the output of household radiators can partly replace that of ACs, although the ratio is needed to be furtherly optimized with proper IDR strategy.

In this paper, the quality of operating reserve includes three aspects, i.e., aggregate capacity, duration, and smoothness. The aggregate capacity of the operating reserve is determined by the reduction of the aggregate power of ACs. FIGURE 2(c) shows that the aggregate power of ACs in part C is large under traditional DR, while FIGURE 2(f) shows that the aggregate power of ACs in part B' is small under IDR. Therefore, the reduction of the aggregate power of ACs is larger, and the aggregate capacity of the operating reserve under IDR is larger than that under traditional DR. The duration of the operating reserve refers to the period that reserve service provides to maintain the required reserve capacity. FIGURE 2(c) shows that the aggregate power of ACs in part c is large, so part c is not considered in the duration of the operating reserve under traditional DR. However, FIGURE 2(f) shows that the aggregate power of ACs in part B' (i.e., part B and C) is small, so part B' is considered in the duration of the operating reserve under IDR. Therefore, the duration of the operating reserve under IDR is longer than that under traditional DR. The smoothness of the operating reserve is related to the rebound effects. FIGURE 2(c) shows that the

**FIGURE 3.** Two-stage IDR strategy.

rebound effects with large power fluctuations occur in part D under traditional DR, while FIGURE 2(f) shows that the rebound effects are mitigated in part C' under IDR since the aggregate power of ACs is reduced by increasing the power consumption of household radiators. Therefore, the operating reserve under IDR is smoother than that under traditional DR. In summary, the quality of operation reserve provided with MTCLs under IDR will improve to some extent.

IV. TWO-STAGE IDR STRATEGY FOR OPERATING RESERVE PROVISION CONSIDERING REBOUND EFFECTS

Based on the expected advantages of IDR analyzed in section III, a two-stage IDR strategy is proposed to fully excavate the operating reserve provided from MTCLs while mitigating rebound effects. The structure of the proposed two-stage IDR strategy is illustrated in FIGURE 3. The first stage is to coordinate the energy consumption of ACs and household radiators to maximize the end-users' thermal comfort and mitigate the rebound effects. Based on the energy consumption results determined in the first stage, the energy conversion in EH is optimized in the second stage. Based on the energy consumption of each device in EH optimized in the second stage, the optimal aggregate energy input from the power system and gas system to EH can be obtained finally.

A. FIRST STAGE: THERMAL COMFORT MAXIMIZATION

The PPD index is an effective measure to predict the thermal comfort of end-users by considering both environmental parameters and personal parameters [29]. The PPD index was proposed to describe the percentage of dissatisfaction for the group of people in the given space [30].

The PPD model can be seen as a function of the room temperature T_v^{in} , as shown in (18).

$$f_{PPD}(T_v^{in}) = 100 - 95 \exp \left[-0.03353 \left[f_{PMV}(T_v^{in}) \right]^4 - 0.2179 \left[f_{PMV}(T_v^{in}) \right]^2 \right] \quad (18)$$

where, $f_{PMV}(T_v^{in})$ is the predicted mean vote (PMV) in room v. The detailed PMV model is referred to [29].

Therefore, (18) can be approximately transformed to (19) by second-order Taylor series expansion to facilitate calculation.

$$\begin{aligned} f_{PPD}(T_v^{in}) &= \frac{f_{PPD}(T_0^{in})}{0!} + \frac{f'_{PPD}(T_0^{in})}{1!} (T_v^{in} - T_v^{comf}) \\ &\quad + \frac{f''_{PPD}(T_0^{in})}{2!} (T_v^{in} - T_v^{comf})^2 \\ &= \theta_1 (T_v^{in} - T_v^{comf})^2 + \theta_2 \end{aligned} \quad (19)$$

where, θ_1, θ_2 are the coefficients of the modified PPD index, which can be determined by the Taylor series. Moreover, the modified PPD index is a quadratic function of the dissatisfaction of end-users, i.e., the difference between the set temperature and comfort temperature. Therefore, the dissatisfaction of end-users is larger, the value of the modified PPD index is larger.

As shown in equations (12)-(17), due to the high correlation between end-users' thermal comfort and rebound effects, it is vital to optimize the end-users' thermal comfort for mitigating the rebound effects, i.e., minimizing the violation of end-users' thermal comfort. Therefore, the objective of the IDR strategy in the first stage is formulated as:

$$\min f_1 = \sum_t \left(\sum_v PPD_v(T_v^{in}(t)) \right) \quad (20)$$

Under the METD model of MTCLs proposed in this paper, the end-users can meet the needs of cooling/heating power by both ACs and household radiators. Therefore, the decision variables of the first stage of IDR strategy are the output and operation status of MTCLs. The constraints of the IDR strategy in the first stage are formulated as: (4)-(6), (21).

$$P_{\Omega, v, -}^{RAD} \leq P_{\Omega, v}^{RAD}(t) \leq P_{\Omega, v, +}^{RAD} \quad (21)$$

where, equation (21) limits the energy generation output of the radiator. $P_{\Omega, v, -}^{RAD}/P_{\Omega, v, +}^{RAD}$ is the lower/upper band of energy output (energy type Ω) of the household radiator to room v.

In this paper, the differential equation (4) can be discretized as equation (22) according to the time step of controlling the set temperature of MTCLs. After each time step, the operation status (on/off) of the compressor of AC and the energy output of the household radiator in each room would be checked or changed.

$$T_v^{in}(t+1) = T_v^{in}(t) + \frac{t_{step}}{C_v} \left(\frac{T_v^{out}(t) - T_v^{in}(t)}{R_v} + m^S P_v(t) \right) \quad (22)$$

where, t_{step} is the time step of controlling the set temperature of MTCLs.

Meanwhile, due to the energy output of the AC and household radiator at time t , the operation status of the compressor of AC is determined by equation (6) at time $t + 1$. This equation determines the energy output of the AC at time $t + 1$ until the end-user change the set temperature or the energy output of household radiators. In this stage of the IDR strategy, the energy consumption of the ACs and household radiators will be optimally dispatched to minimize the modified PPD index in every room at each time and sent to the second stage of the IDR strategy.

B. SECOND STAGE: OPERATION COST MINIMIZATION

Based on the energy consumption of ACs and household radiators of end-users optimal dispatched in the first stage of IDR strategy, the aggregated multi-energy loads of EH can be figured as the sum of these MTCLs and the rest loads, as shown in equation (11). In the second stage of the IDR strategy, the objective function is to minimize the operation cost of EH, including electricity and natural gas costs. The multi-energy output of the devices in EH, as the decision variables of the second stage of IDR strategy, is optimized for the minimum operating cost, as shown in equation (23).

$$\min f_2 = \sum_{\Omega} \left(c_{\Omega} \times \sum_t \left(\sum_i P_{\Omega,ji}^{out}(t) + \xi \sum_i \beta_{\Omega}^i(t) \right) \right), \quad j = 0 \quad (23)$$

Subject to: (9)-(11), (24)-(27)

$$P_{\Omega,i,-}^{out} \leq P_{\Omega,i}^{out}(t) - \beta_{\Omega}^i(t) \leq P_{\Omega,i,+}^{out}, \quad i \in \{2, 3, 4, 5\} \quad (24)$$

$$P_{\Omega,i,-}^{ramp} \leq P_{\Omega,i}^{out}(t) - \beta_{\Omega}^i(t) - P_{\Omega,i}^{out}(t-1) + \beta_{\Omega}^i(t-1) \leq P_{\Omega,i,+}^{ramp} \quad (25)$$

$$\begin{cases} P_{H,1}^{out}(t) - \beta_H^1(t) \geq 0 \\ P_{E,1}^{out}(t) - P_{E,1}^A - \frac{P_{E,1}^A - P_{E,1}^B}{P_{H,1}^A - P_{H,1}^B} \times (P_{H,1}^{out}(t) - \beta_H^1(t)) \leq 0 \\ P_{E,1}^{out}(t) - P_{E,1}^B - \frac{P_{E,1}^B - P_{E,1}^C}{P_{H,1}^B - P_{H,1}^C} \times (P_{H,1}^{out}(t) - \beta_H^1(t) - P_{H,1}^B) \geq 0 \\ P_{E,1}^{out}(t) - P_{E,1}^D - \frac{P_{E,1}^C - P_{E,1}^D}{P_{H,1}^C - P_{H,1}^D} \times (P_{H,1}^{out}(t) - \beta_H^1(t)) \geq 0 \\ \beta_{\Omega}^i(t) \geq 0 \end{cases} \quad (26)$$

where, equation (24) limits the energy generation output on devices of the EH. Equation (25) limits the energy ramp rate on devices of the EH. $P_{\Omega,1}^A, P_{\Omega,1}^B, P_{\Omega,1}^C, P_{\Omega,1}^D$ ($\Omega \in \{E, H\}$) are extreme points forming the feasible operating region of the CHP. $P_{\Omega,i,-}^{out}/P_{\Omega,i,+}^{out}$ is the lower/upper band of energy capacity (energy type Ω) of the device i . $P_{\Omega,i,+}^{ramp}/P_{\Omega,i,-}^{ramp}$ is the

lower/upper band of energy ramp rate (energy type Ω) of the device i . c_{Ω} is the unit price of Ω . Equation (26) represents the convex feasible operating region of the CHP. In equation (27), β_{Ω}^i is the slack variable (energy type Ω) of the device i . ξ is a penalty factor.

Note that the upper band of energy output (energy type Ω) of the household radiator in equation (21) does not only depend on the product model but also the limits of energy generation output on devices of the EH, as shown in equation (28).

$$\sum_v P_{\Omega,v,+}^{RAD} \leq \sum_v P_{\Omega,v,n}^{RAD} - \sum_i \beta_{\Omega}^i, \quad \Omega \in \{C, H\} \quad (28)$$

where, $P_{\Omega,v,n}^{RAD}$ is the maximum energy output (energy type Ω) of the household radiator, determined on the product model.

Based on the energy output of the ACs and household radiators optimized in the first stage of IDR strategy, if $\beta_{\Omega}^i \neq 0$, it means the optimal output of device i is overwhelming and has to be set as its upper band. The second stage of the IDR strategy will have no solution. Therefore, the first stage of IDR strategy needs to be optimized again based on the equation (28) to make sure this two-stage of IDR strategy has a feasible solution, as shown in FIGURE 3.

V. EFFECTIVENESS EVALUATION OF THE PROPOSED IDR METHOD

By solving the proposed two-stage IDR strategy in Section IV, the operating reserve provided from MTCLs can be calculated. In order to evaluate the quality of operating reserve, multidimensional evaluation indices are introduced in this section.

A. OPERATING RESERVE QUALITY EVALUATION

1) AGGREGATE CAPACITY

The aggregate capacity of the operating reserve can be formulated as the sum of the difference of electrical loads between the original status and after IDR [5], as shown in equation (29).

$$E_{ORC} = \sum_t \left(\sum_i P_{\Omega,ji}^{out}(t) - P_{\Omega}^0(t) \right), \quad j = 0, \quad \Omega = E \quad (29)$$

where, E_{ORC} is the aggregate capacity of operating reserve in power systems. $P_{\Omega}^0(t)$ is the original electrical loads.

2) DURATION

The duration of the operating reserve refers to the period that reserve service provides to maintain the required reserve capacity [7]. The duration index is the ratio of duration time to the whole DR time, as shown in equation (30).

$$E_{ORD} = \frac{t_{DR}^d}{t_{DR}^e - t_{DR}^s} \quad (30)$$

where, E_{ORD} is the duration index of operating reserve in power systems.

TABLE 4. Capacities of the devices in the test system (kW).

$P_{H,1}^A$	$P_{E,1}^A$	$P_{H,1}^B$	$P_{E,1}^B$	$P_{H,1}^C$	$P_{E,1}^C$
0	2500	1100	2100	900	500
$P_{H,1}^D$	$P_{E,1}^D$	$P_{H,2,-}^{out}$	$P_{H,2,+}^{out}$	$P_{H,3,-}^{out}$	$P_{H,3,+}^{out}$
0	1000	200	2500	200	2500
$P_{C,4,-}^{out}$	$P_{C,4,+}^{out}$	$P_{C,5,-}^{out}$	$P_{C,5,+}^{out}$	$P_{C,v,-}^{EH}$	$P_{C,v,+}^{EH}$
200	4500	0	3000	0	2

TABLE 5. Ramp rate of the devices in the test system (kW/s).

$P_{H,1,-}^{ramp}$	$P_{H,1,+}^{ramp}$	$P_{E,1,-}^{ramp}$	$P_{E,1,+}^{ramp}$	$P_{H,2,-}^{ramp}$	$P_{H,2,+}^{ramp}$
-739.2	739.2	-554.4	554.4	-2000	2000
$P_{H,3,-}^{ramp}$	$P_{H,3,+}^{ramp}$	$P_{C,4,-}^{ramp}$	$P_{C,4,+}^{ramp}$	$P_{C,5,-}^{ramp}$	$P_{C,5,+}^{ramp}$
-1250	1250	-18000	18000	-6000	6000

3) SMOOTHNESS

The smoothness of operating reserve can be quantified as the peak capacity of rebound effects, which is the maximum power difference between the original status and after IDR [22], as shown in equation (31).

$$E_{ORS} = \max \left(\sum_i P_{\Omega,ji}^{out}(t) - P_{\Omega}^0(t) \right), \quad t \geq t_{DR}^s, \\ j = 0, \quad \Omega = E \quad (31)$$

where, E_{ORS} is the smoothness of operating reserve.

B. THERMAL COMFORT EVALUATION OF END-USERS

Based on the modified PPD index, the thermal comfort can be quantitatively evaluated as:

$$E_{comf} = \sum_t \left(\sum_i PPD_v(t) - PPD_v^0(t) \right) \quad (32)$$

where, E_{comf} is the thermal comfort violation.

VI. CASE STUDIES

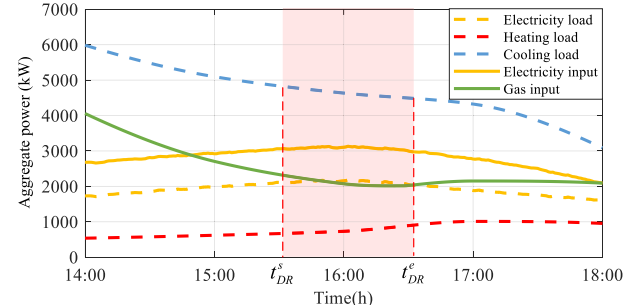
A. TEST SYSTEM AND PARAMETERS

The test system is a typical and widely-used multi-energy system [27]–[33], which is connected to a load node of an electrical system. The structure of the multi-energy system is shown as FIGURE 1. The data of the devices such as air conditioners (ACs), combined heat and power plants, and electricity boilers in the multi-energy system come from realistic cases. Specifically, the capacities of the devices, the ramp rate of the devices, and the detailed parameters of the end-users, are presented in TABLE 4, TABLE 5, and TABLE 6, respectively. The operation parameters of EH are referred to [31]. The operation parameters of ACs are generated from a pilot study that obtains spinning reserve from responsive air conditioning loads at a motel over a year [32]. The coefficient of performance COP of ACs is set according to [5]. Thermal parameters of rooms are set according to [27]. The hypothetical electricity, heating and cooling loads for the EH on a selected summer day are presented in FIGURE 4 [33].

TABLE 6. AC physical parameters, taylor series coefficients of PPD and unit price.

v	A_v	C_v	R_v	COP_v^{AC}	P_v^{AC}
	(m^2)	($kWh / ^\circ C$)	($^\circ C / kW$)		(kW)
200	$N(25,30)$	$0.015 \cdot A_v$	$100 \cdot A_v^{-1}$	3.9051	$U(1,2)$
T_v^{set}	ΔT_v^{DR}	θ_1	θ_2	c_E	c_G
($^\circ C$)	($^\circ C$)			(\$)	(\$)
$U(23,26)$	2	0.7022	4.94	80	48

Normal distribution with the mean value of μ and the standard deviation of σ is abbreviated to $N(\mu, \sigma^2)$; uniform distribution with the minimum and maximum value of a and b , respectively, is abbreviated to $U(a, b)$.

**FIGURE 4.** The hypothetical energy loads and energy input.**TABLE 7.** Simulation results of three cases in the test system.

	the violation of end-users' thermal comfort f_1	operation cost f_2 (\$)
Case 1	2.418×10^5	830×10^5
Case 2	2.678×10^5	828×10^5
Case 3	2.423×10^5	844×10^5

As FIGURE 4 indicates, comparing the cooling load in summer, the heating loads stay at a relatively low level. It can be observed that the cooling load generally declines and the gas input of the EH is in a decreasing trend during 14:00 - 18:00. In addition to the decline of gas input, the electric system's peak load exists at around 16:00. Therefore, ACs are dispatched to provide load-reduction service during 15:30 - 16:30.

B. CALCULATED RESULTS

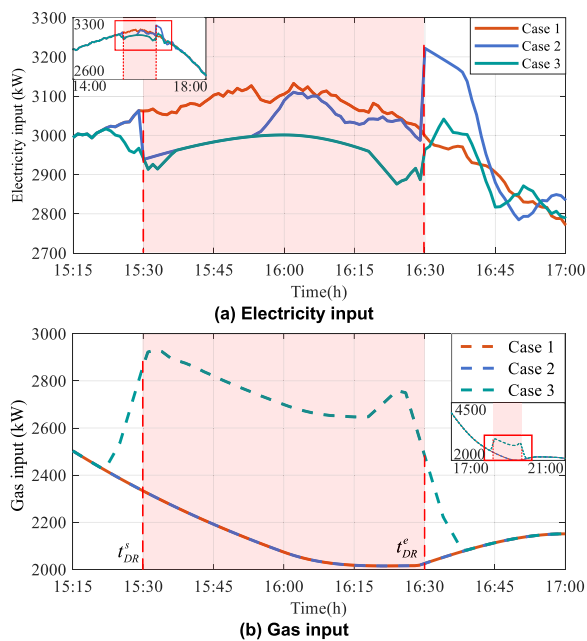
In order to illustrate the benefits of the proposed two-stage IDR strategy, three cases are designed in this paper which includes:

- 1) Case 1 has no-DR strategy, where the operation of EH devices is dispatched normally and end-users' devices are in operation based on user preferences.
- 2) Case 2 is a traditional DR strategy utilized widely in many countries [7], where only ACs participate in DR programs.
- 3) Case 3 applied the proposed two-stage IDR strategy of MTCLs, where end-users' thermal comfort can be satisfied by both ACs and household radiators.

The simulation results of the three cases are as shown in TABLE 7 and TABLE 8. Due to the set temperature

TABLE 8. Evaluation results of three cases in the test system.

E_{ORC} (kW)	t_{DR}^d (min)	E_{ORD} (kW)	E_{ORS} (kW)	E_{comf} ($\times 10^4$)
--	--	--	--	--
Case 1	--	--	--	--
Case 2	3813	23	38.33%	232.6
Case 3	7051	60	100%	119.4
				1.73

**FIGURE 5.** Energy input of the test system.

control of ACs in the contract of DR program, Case 2 has a slight reduction compared to the original operating cost, from $830 \times 10^5 \$$ to $828 \times 10^5 \$$. Due to the growth of gas power, the operating cost of Case 3 is the highest in the three cases, reaching $844 \times 10^5 \$$. There is no denying that, on the operating cost, the proposed two-stage IDR strategy of MTCLs is more expensive than the traditional DR program. However, considering the cost of the subsidy and thermal comfort violation of end-users, which is set as 40 \$ [28], the total cost of the test system in Case 3 ($940.92 \times 10^5 \$$) just has a little increase than Case 2 ($935.12 \times 10^5 \$$).

1) RESERVE RESOURCE QUALITY ANALYSIS

In Case 1, in order to set the baseline for implementing the scheduling, the traditional DR or IDR program is not implemented and the results of multi-energy flow are illustrated in FIGURE 5.

The aggregative multi-energy input profile in different dispatch strategies is illustrated in FIGURE 5(a)-(b). The electricity input profile of Case 2 in FIGURE 5(a) shows that the aggregative electricity has a recovery at time 15:50. As shown in TABLE 8, the recovery appears at 23 minutes after the IDR start time. It can be observed that the electricity input of the test system in Case 2 is slightly lower than Case 1, which is part C in the METD model. This situation means

the expected operating reserve in power systems provided by ACs is not prominent during this period. As shown in TABLE 8, the duration index E_{ORD} increases from 38.33% in Case 2 to 100% in Case 3. Therefore, the proposed IDR strategy can provide a longer duration of operating reserve than the traditional DR program.

As shown in FIGURE 5(a), the rebound effects appear at the end of the DR period, which is much higher than the original electricity input peak in power systems and lasts about 15 minutes. This electricity input peak is 3221.8 kW. Meanwhile, this short and huge electricity peak cannot be mitigated by the devices of EH because of the limitation of the ramp rate. So, the gas input of the test system in Case 2 is the same as Case 1. On the other hand, in Case 3, the MTCLs are required to provide operating reserve with a specified duration time (15:30 – 16:30). As discussed in Section II, the EH will provide extra cooling input of the end-user directly by household radiators, as shown in FIGURE 1. The multi-energy input profile of Case 3 in FIGURE 5(b) shows the extra cooling input of end-users provided by both electricity and gas. As FIGURE 5(a) indicates, it can be observed that the electricity input is mitigated during the IDR period (15:30 – 16:30) in Case 3. Besides, the rebound effects have a significant reduction after the IDR period. The electricity input peak is 3041.4 kW in Case 3, which is much lower than that in Case 2. Moreover, TABLE 8 shows the smoothness improves from 232.6 kW to 119.4 kW. The rebound effects are mitigated due to the less violation of the end-user thermal comfort. Therefore, the proposed IDR strategy can provide a smoother operating reserve than the traditional DR program.

On the other hand, in Case 3, the aggregate capacity of operating reserve in power systems is 7051 kW, which is much higher than Case 2 (3813 kW) as shown in TABLE 8. Therefore, the proposed IDR strategy can provide a higher aggregate capacity of operating reserve than the traditional DR program. Moreover, the ramp time of ACs is set as 0.21 min, which is referred to [5]. Based on it, the ramp rate of operating reserve provided by the proposed IDR strategy is 9.7 kW/s. The ramp rate of the operating reserve will have no distinct difference between the proposed IDR strategy and the traditional DR program, which meets the requirement of power systems.

Therefore, the proposed IDR strategy can provide a long-duration, high-aggregate-capacity operating reserve and mitigate the rebound effects.

2) END-USERS' THERMAL COMFORT ANALYSIS

The room temperature of end-users of three cases is as shown in FIGURE 6. In Case 1, every AC's set temperature is end-users' thermal comfort temperature and in normal operation status, as shown in FIGURE 6(a). In Case 2, the set temperature of ACs will change and be away from thermal comfort temperature according to DR contracts during the DR period. Therefore, the room temperature will be near to ambient temperature until it reaches the set temperature of the IDR contracts. The difference between some end-users'

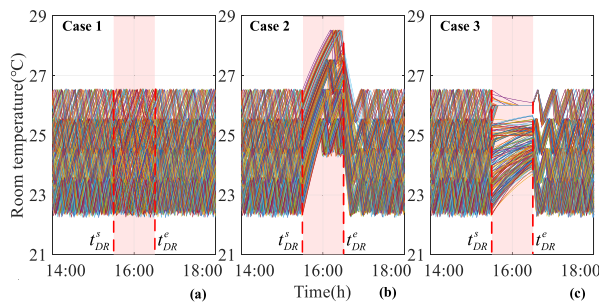


FIGURE 6. Room temperature versus time under different cases.

thermal comfort temperature and ambient temperature is large, so these ACs will operate earlier than others, as shown in FIGURE 6(b). In Case 3, due to the output of household radiators, the room temperature is much more near to end-users' thermal comfort temperature with the proposed IDR strategy than the traditional DR program. Because of the difference between end-users' thermal comfort temperature and ambient temperature, some end-users will stay in their thermal comfort temperature and others will also be nearer to their thermal comfort temperature than Case 2, as shown in FIGURE 6(c).

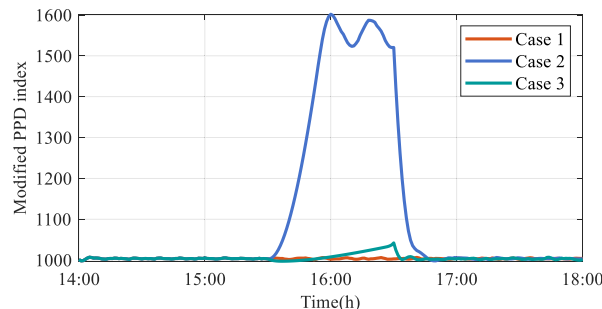


FIGURE 7. Values of modified PPD index under different cases.

The modified PPD index of three cases, which quantifies the end-user comfort violation, is as shown in FIGURE 7. Traditional DR program has much more violation of end-users' thermal comfort in Case 2 than Case 3. These simulation results are consistent with the room temperature in FIGURE 6. Besides, E_{comf} decreases from 103.2 (Case 2) to 1.73 (Case 3), as shown in TABLE 8.

Therefore, the end-users' thermal comfort with the proposed IDR strategy can be much higher than the traditional DR program.

C. DISCUSSION

Numerical results show that the proposed IDR strategy can provide a higher aggregate capacity of operating reserve than the traditional DR program since the capacity index E_{ORD} in Case 3 is 1.85 times that in Case 2. The duration index E_{ORD} in Case 3 is 2.61 times that in Case 2, indicating that the proposed IDR strategy can provide a longer duration of operating reserve. As for the smoothness, the capacity of rebound effects is reduced from 232.6 kW in Case 2 to

119.4kW in Case 3, so the proposed IDR strategy can provide a smoother operating reserve than the traditional DR program. Besides, the thermal comfort index E_{comf} decreases from 103.2 (Case 2) to 1.73 (Case 3), meaning that the end-users' thermal comfort by the proposed IDR strategy is much higher than the traditional DR program. In summary, the proposed two-stage IDR strategy can provide high-aggregate-capacity and long-duration reserve resources in power systems while mitigating the rebound effects.

Moreover, we have validated the proposed method from two aspects. 1) Firstly, the proposed two-stage IDR strategy includes two models, i.e., the METD model and the EH model. The METD model is a classic model to describe the relationship between the room temperature and the output of TCLs, whose validity has been proved in Section II. The EH model is a classic model to describe the energy conversion among different devices including the CHP, the EB, the GB, and the AB. The operation parameters of these devices are referred to real systems, whose validity has been proved in many references [28]–[33]. 2) Moreover, based on the METD model and EH model, the two-stage IDR strategy is formulated as a mixed-integer linear programming problem. The feasible region of the proposed strategy can be convex which can converge to the globally optimal solution. Besides, the calculation results of the test system by Cplex solver and Gurobi solver are consistent, which can also validate the proposed method.

VII. CONCLUSION

With the introduction of EHs, the IDR strategies provide a new perspective to enhance the operating reserve of power systems. This paper proposes a two-stage IDR strategy to fully excavate the operating reserve provided from MTCLs considering rebound effects. Illustrative results demonstrate that the proposed two-stage IDR strategy can provide high-aggregate-capacity and long-duration reserve resources in power systems while mitigating the rebound effects. The thermal comfort violation of end-users can be minimized, close to the original most comfortable status.

Moreover, the proposed strategy has some implications for research, practice, and society. Firstly, a novel IDR strategy is proposed in this paper to excavate the operating reserve of multi-energy loads, which can provide methods for the scheduling of other demand response resources, e.g., multi-energy storages. Besides, the proposed model can ensure thermal comforts, which will significantly encourage end-users to participate in demand response programs. Considering that, the power grid companies can obtain more operating reserve resources to guarantee the supply-demand balance. Moreover, the proposed model can postpone the construction of other adjusting resources for the accommodation of renewable energy, which can accelerate the low-carbon and economic development of society.

Furthermore, this paper focuses on the demand side and the multi-energy system studied is connected to load nodes of

electrical and gas systems. The proposed two-stage IDR strategy can provide high-aggregate-capacity and long-duration reserve resources while mitigating the rebound effects to maintain supply-demand balance and reliable operation of power systems. Taking full account of detailed models of electrical and gas systems in the proposed IDR strategy can help to excavate the operating reserve provision more precisely. However, due to the space limitation of this paper, the detailed models of electrical and gas systems are not considered. The IDR strategy considering the detailed model of the electrical and gas systems will be studied in the future.

REFERENCES

- [1] (2021). *Accelerating the Transition From Coal to Clean Power*. [Online]. Available: <https://ukcop26.org/energy/>
- [2] P. Nikolaidis, S. Chatzis, and A. Poullikkas, "Optimal planning of electricity storage to minimize operating reserve requirements in an isolated island grid," *Energy Syst.*, vol. 11, no. 4, pp. 1157–1174, Nov. 2020, doi: [10.1007/s12667-019-00355-x](https://doi.org/10.1007/s12667-019-00355-x).
- [3] Y. Ding, W. Cui, S. Zhang, H. Hui, Y. Qiu, and Y. Song, "Multi-state operating reserve model of aggregate thermostatically-controlled-loads for power system short-term reliability evaluation," *Appl. Energy*, vol. 241, pp. 46–58, May 2019, doi: [10.1016/j.apenergy.2019.02.018](https://doi.org/10.1016/j.apenergy.2019.02.018).
- [4] Ž. B. Rejc and M. Čepin, "Estimating the additional operating reserve in power systems with installed renewable energy sources," *Int. J. Electr. Power Energy Syst.*, vol. 62, pp. 654–664, Nov. 2014, doi: [10.1016/j.ijepes.2014.05.019](https://doi.org/10.1016/j.ijepes.2014.05.019).
- [5] H. Hui, Y. Ding, W. Liu, Y. Lin, and Y. Song, "Operating reserve evaluation of aggregated air conditioners," *Appl. Energy*, vol. 196, pp. 218–228, Jun. 2017, doi: [10.1016/j.apenergy.2016.12.004](https://doi.org/10.1016/j.apenergy.2016.12.004).
- [6] H. Zhong, Q. Xia, C. Kang, M. Ding, J. Yao, and S. Yang, "An efficient decomposition method for the integrated dispatch of generation and load," *IEEE Trans. Power Syst.*, vol. 30, no. 6, pp. 2923–2933, Nov. 2015, doi: [10.1109/TPWRS.2014.2381672](https://doi.org/10.1109/TPWRS.2014.2381672).
- [7] H. Hui, Y. Ding, Z. Lin, P. Siano, and Y. Song, "Capacity allocation and optimal control of inverter air conditioners considering area control error in multi-area power systems," *IEEE Trans. Power Syst.*, vol. 35, no. 1, pp. 332–345, Jan. 2020, doi: [10.1109/TPWRS.2019.2924348](https://doi.org/10.1109/TPWRS.2019.2924348).
- [8] V. Trovato, F. Teng, and G. Strbac, "Role and benefits of flexible thermostatically controlled loads in future low-carbon systems," *IEEE Trans. Smart Grid*, vol. 9, no. 5, pp. 5067–5079, Sep. 2018, doi: [10.1109/TSG.2017.2679133](https://doi.org/10.1109/TSG.2017.2679133).
- [9] H. W. Chon, M. Beaudin, H. Zareipour, A. Schellenberg, and L. Ning, "Cooling devices in demand response: A comparison of control methods," *IEEE Trans. Smart Grid*, vol. 6, no. 1, pp. 249–260, Jan. 2015, doi: [10.1109/TSG.2014.2358579](https://doi.org/10.1109/TSG.2014.2358579).
- [10] S. Bahrami and A. Sheikhi, "From demand response in smart grid toward integrated demand response in smart energy hub," *IEEE Trans. Smart Grid*, vol. 7, no. 2, pp. 650–658, Mar. 2016, doi: [10.1109/TSG.2015.2464374](https://doi.org/10.1109/TSG.2015.2464374).
- [11] K. P. Schneider, E. Sortomme, S. S. Venkata, M. T. Miller, and L. Ponder, "Evaluating the magnitude and duration of cold load pick-up on residential distribution feeders_newline using multi-state load models," *IEEE Trans. Power Syst.*, vol. 31, no. 5, pp. 3765–3774, Sep. 2016, doi: [10.1109/TPWRS.2015.2494882](https://doi.org/10.1109/TPWRS.2015.2494882).
- [12] C. Wouters, E. S. Fraga, and A. M. James, "An energy integrated, multi-microgrid, MILP (mixed-integer linear programming) approach for residential distributed energy system planning—A south Australian case-study," *Energy*, vol. 85, pp. 30–44, Jun. 2015, doi: [10.1016/j.energy.2015.03.051](https://doi.org/10.1016/j.energy.2015.03.051).
- [13] C. Chen, X. Deng, Z. Zhang, S. Liu, M. Waseem, Y. Dan, Z. Lan, Z. Lin, L. Yang, and Y. Ding, "Optimal day-ahead scheduling of multiple integrated energy systems considering integrated demand response, cooperative game and virtual energy storage," *IET Gener. Transmiss. Distrib.*, vol. 15, no. 11, pp. 1657–1673, Feb. 2021, doi: [10.1049/gtd2.12124](https://doi.org/10.1049/gtd2.12124).
- [14] J. Wang, H. Zhong, Z. Ma, Q. Xia, and C. Kang, "Review and prospect of integrated demand response in the multi-energy system," (in English), *Appl. Energy*, vol. 202, pp. 772–782, Sep. 2017, doi: [10.1016/j.apenergy.2017.05.150](https://doi.org/10.1016/j.apenergy.2017.05.150).
- [15] Z. Jiang, Q. Ai, and R. Hao, "Integrated demand response mechanism for industrial energy system based on multi-energy interaction," *IEEE Access*, vol. 7, pp. 66336–66346, 2019, doi: [10.1109/ACCESS.2019.2917821](https://doi.org/10.1109/ACCESS.2019.2917821).
- [16] L. Wang, C. Hou, B. Ye, X. Wang, C. Yin, and H. Cong, "Optimal operation analysis of integrated community energy system considering the uncertainty of demand response," *IEEE Trans. Power Syst.*, vol. 36, no. 4, pp. 3681–3691, Jul. 2021, doi: [10.1109/TPWRS.2021.3051720](https://doi.org/10.1109/TPWRS.2021.3051720).
- [17] P. Li, Z. Wang, N. Wang, W. Yang, M. Li, X. Zhou, Y. Yin, J. Wang, and T. Guo, "Stochastic robust optimal operation of community integrated energy system based on integrated demand response," *Int. J. Electr. Power Energy Syst.*, vol. 128, Jun. 2021, Art. no. 106735, doi: [10.1016/j.ijepes.2020.106735](https://doi.org/10.1016/j.ijepes.2020.106735).
- [18] Y. Li, C. Wang, G. Li, and C. Chen, "Optimal scheduling of integrated demand response-enabled integrated energy systems with uncertain renewable generations: A Stackelberg game approach," *Energy Convers. Manage.*, vol. 235, May 2021, Art. no. 113996, doi: [10.1016/j.enconman.2021.113996](https://doi.org/10.1016/j.enconman.2021.113996).
- [19] J. Wang, K.-J. Li, Y. Liang, and Z. Javid, "Optimization of multi-energy microgrid operation in the presence of PV, heterogeneous energy storage and integrated demand response," *Appl. Sci.*, vol. 11, no. 3, pp. 1–20, 2021, doi: [10.3390/app11031005](https://doi.org/10.3390/app11031005).
- [20] H. Yang, T. Xiong, and J. Qiu, "Optimal operation of DES/CCHP based regional multi-energy prosumer with demand response," *Appl. Energy*, vol. 167, pp. 353–365, Apr. 2016, doi: [10.1016/j.apenergy.2015.11.022](https://doi.org/10.1016/j.apenergy.2015.11.022).
- [21] S. Zheng, Y. Sun, B. Li, B. Qi, X. Zhang, and F. Li, "Incentive-based integrated demand response for multiple energy carriers under complex uncertainties and double coupling effects," *Appl. Energy*, vol. 283, Feb. 2021, Art. no. 116254, doi: [10.1016/j.apenergy.2020.116254](https://doi.org/10.1016/j.apenergy.2020.116254).
- [22] W. Cui, Y. Ding, H. Hui, Z. Lin, P. Du, Y. Song, and C. Shao, "Evaluation and sequential dispatch of operating reserve provided by air conditioners considering lead-lag rebound effect," *IEEE Trans. Power Syst.*, vol. 33, no. 6, pp. 6935–6950, Nov. 2018, doi: [10.1109/TPWRS.2018.2846270](https://doi.org/10.1109/TPWRS.2018.2846270).
- [23] E. Merkel, R. McKenna, and W. Fichtner, "Optimisation of the capacity and the dispatch of decentralised micro-CHP systems: A case study for the U.K.," *Appl. Energy*, vol. 140, pp. 120–134, Feb. 2015, doi: [10.1016/j.apenergy.2014.11.036](https://doi.org/10.1016/j.apenergy.2014.11.036).
- [24] M. Ameri and Z. Besharati, "Optimal design and operation of district heating and cooling networks with CCHP systems in a residential complex," *Energy Buildings*, vol. 110, pp. 135–148, Jan. 2016, doi: [10.1016/j.enbuild.2015.10.050](https://doi.org/10.1016/j.enbuild.2015.10.050).
- [25] L. Li, H. Mu, W. Gao, and M. Li, "Optimization and analysis of CCHP system based on energy loads coupling of residential and office buildings," *Appl. Energy*, vol. 136, pp. 206–216, Dec. 2014, doi: [10.1016/j.apenergy.2014.09.020](https://doi.org/10.1016/j.apenergy.2014.09.020).
- [26] F. Salata, A. de Lieto Vollaro, R. de Lieto Vollaro, and L. Mancieri, "Method for energy optimization with reliability analysis of a trigeneration and teleheating system on urban scale: A case study," *Energy Buildings*, vol. 86, pp. 118–136, Jan. 2015, doi: [10.1016/j.enbuild.2014.09.056](https://doi.org/10.1016/j.enbuild.2014.09.056).
- [27] D. S. Callaway, "Tapping the energy storage potential in electric loads to deliver load following and regulation, with application to wind energy," *Energy Convers. Manage.*, vol. 50, no. 5, pp. 1389–1400, May 2009, doi: [10.1016/j.enconman.2008.12.012](https://doi.org/10.1016/j.enconman.2008.12.012).
- [28] S. Ye, W. Ruan, S. Wang, and C. Zhang, "A bi-level equivalent model of scheduling an energy hub to provide operating reserve for power systems," in *Proc. Tsinghua HUST-IET Electr. Eng. Academic Forum*, 2020, pp. 1–7.
- [29] K. Ma, Y. Yu, B. Yang, and J. Yang, "Demand-side energy management considering price oscillations for residential building heating and ventilation systems," *IEEE Trans. Ind. Informat.*, vol. 15, no. 8, pp. 4742–4752, Aug. 2019, doi: [10.1109/TII.2019.2901306](https://doi.org/10.1109/TII.2019.2901306).
- [30] K. Fabbri, "The indices of feeling-predicted mean vote PMV and percentage people dissatisfied PPD," in *Indoor Thermal Comfort Perception: A Questionnaire Approach Focusing Children*, K. Fabbri, Ed. Cham, Switzerland: Springer, 2015, pp. 75–125.
- [31] P. Mancarella and G. Chicco, "Real-time demand response from energy shifting in distributed multi-generation," *IEEE Trans. Smart Grid*, vol. 4, no. 4, pp. 1928–1938, Dec. 2013, doi: [10.1109/TSG.2013.2258413](https://doi.org/10.1109/TSG.2013.2258413).
- [32] B. J. Kirby and M. R. Ally, "Spinning reserves from controllable packaged through the wall air conditioner (PTAC) units," Tech. Rep., 2003.
- [33] I. G. Moghaddam, M. Saniei, and E. Mashhour, "A comprehensive model for self-scheduling an energy hub to supply cooling, heating and electrical demands of a building," *Energy*, vol. 94, pp. 157–170, Jan. 2016, doi: [10.1016/j.energy.2015.10.137](https://doi.org/10.1016/j.energy.2015.10.137).

• • •